Alanine Scanning Mutagenesis of the Testosterone Binding Site of Rat 3α-Hydroxysteroid Dehydrogenase Demonstrates Contact Residues Influence the Rate-Determining Step†

Vladi V. Heredia,‡ William C. Cooper,§ Ryan G. Kruger,§ Yi Jin,§ and Trevor M. Penning*,§

Departments of Biochemistry and Biophysics and of Pharmacology, University of Pennsylvania School of Medicine, Philadelphia, Pennsylvania 19104

Received January 5, 2004; Revised Manuscript Received March 9, 2004

ABSTRACT: Aldo-keto reductase (AKR1C) isoforms can regulate ligand access to nuclear receptors by acting as hydroxysteroid dehydrogenases. The principles that govern steroid hormone binding and steroid turnover by these enzymes were analyzed using rat 3α-hydroxysteroid dehydrogenase (3α-HSD, AKR1C9) as the protein model. Systematic alanine scanning mutagenesis was performed on the substrate-binding pocket as defined by the crystal structure of the 3α-HSD·$NADP^+$·testosterone ternary complex. T24, L54, F118, F129, T226, W227, N306, and Y310 were individually mutated to alanine, while catalytic residues Y55 and H117 were unaltered. The effects of these mutations on the ordered bi-bi mechanism were examined. No mutations changed the affinity for NADPH by more than 2−3-fold. Fluorescence titrations of the energy transfer band of the E·NADPH complex with competitive inhibitors testosterone and progesterone showed that the largest effect was a 23-fold decrease in the affinity for progesterone in the W227A mutant. By contrast, changes in the K_d for testosterone were negligible. Examination of the k_{cat}/K_m data for these mutants indicated that, irrespective of steroid substrate, the bimolecular rate constant was more adversely affected when alanine replaced an aromatic hydrophobic residue. By far, the greatest effects were on k_{cat} (decreases of more than 2 log units), suggesting that the rate-determining step was either altered or slowed significantly. Single- and multiple-turnover experiments for androsterone oxidation showed that while the wild-type enzyme demonstrated a k_{lim} and burst kinetics consistent with slow product release, the W227A and F118A mutants eliminated this kinetic profile. Instead, single- and multiple-turnover experiments gave k_{lim} and k_{max} values identical with k_{cat} values, respectively, indicating that chemistry was now rate-limiting overall. Thus, conserved residues within the steroid-binding pocket affect k_{cat} more than K_d by influencing the rate-determining step of steroid oxidation. These findings support the concept of enzyme catalysis in which the correct positioning of reactants is essential; otherwise, k_{cat} will be limited by the chemical event.

Steroid target tissues regulate the amount of ligand that is available to bind and transactivate steroid receptors (*1*, *2*). Enzymes that control local steroid hormone concentrations include the 5α/5β-reductases, the steroid sulfatases/sulfotransferases, and the hydroxysteroid dehydrogenases (HSDs). For example, in the prostate, testosterone[1] is converted by 5α-reductase type 2 to the potent androgen 5α-dihydrotestosterone (5α-DHT) (*3*) which is eliminated as 3α-androstanediol by 3α-HSD type 3 (*4*). These classes of enzymes are attractive drug targets because their inhibition regulates the amount of ligand that is available for steroid hormone receptors and can lead to tissue specific hormone responses. Detailed structure−function studies are needed to understand how these enzymes catalyze steroid hormone transformation.

Crystal structures exist for several pertinent enzymes that control ligand access to nuclear receptors. The structure of the murine estrogen sulfotransferase·PAP·estradiol complex (*5*) has been reported. In addition, the HSDs involved in this process belong to two protein superfamilies, the short-chain dehydrogenase/reductases (SDRs) and the aldo-keto reductases (AKRs). Structures of HSDs in both families exist. The human 17β-HSD type 1·$NADP^+$·estradiol complex (*6*, *7*) is representative of the SDRs, and the rat 3α-HSD·$NADP^+$·testosterone complex (*8*) can be used as a protein model for the remaining AKRs. While the existing structures provide vivid three-dimensional models of their respective steroid binding sites, they do not address the individual contribution of each contact residue to steroid binding affinity, specificity, or steroid turnover. To gain insight into these issues, we have conducted an alanine scanning mutagenesis study of the

† This work was supported by NIH Grant DK47015 to T.M.P., and V.V.H. was supported by Structural Biology Training Grant GM08275.

* To whom correspondence should be addressed: Department of Pharmacology, University of Pennsylvania School of Medicine, 135 John Morgan Building, 3620 Hamilton Walk, Philadelphia, PA 19104-6084. Telephone: (215) 898-9445. Fax: (215) 573-2236. E-mail: penning@pharm.med.upenn.edu.

‡ Department of Biochemistry and Biophysics.

§ Department of Pharmacology.

[1] Abbreviations: AKR, aldo-keto reductase; 3α-HSD, 3α-hydroxysteroid dehydrogenase (EC 1.1.1.213, A-face specific and now designated AKR1C9); $NAD(P)^+$, nicotinamide adenine dinucleotide (phosphate); PAP, adenosine 3′,5′-diphosphate; androsterone, 3α-hydroxy-5α-androstan-17-one; testosterone, 17β-hydroxyandrost-4-en-3-one; progesterone, pregn-4-en-3,20-dione; WT, wild-type.

10.1021/bi0499563 CCC: $27.50
Published on Web 04/22/2004

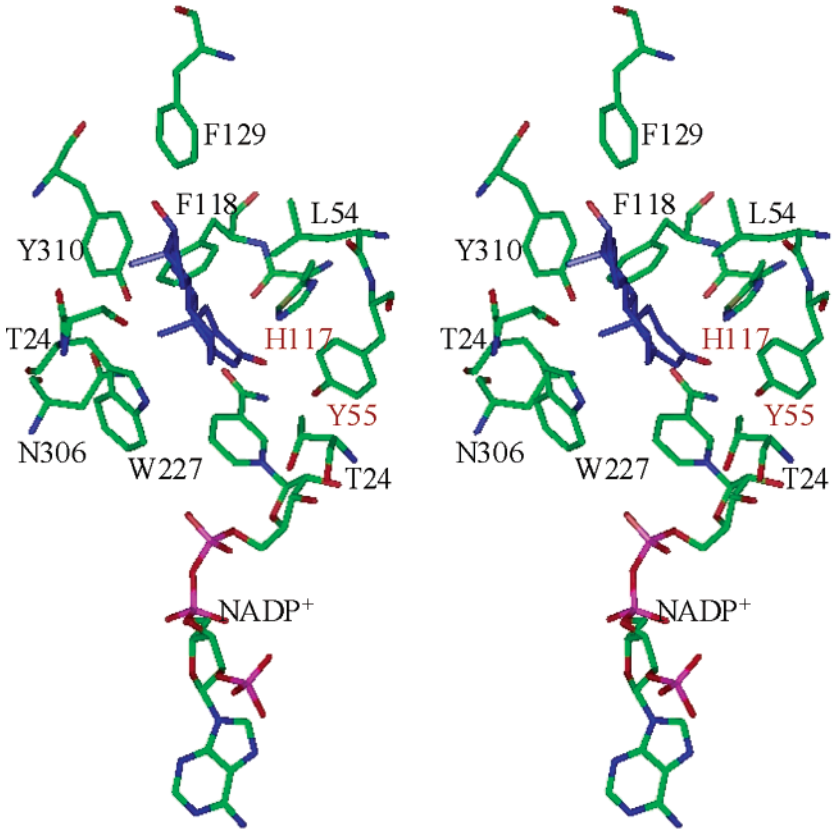

FIGURE 1: Residues that line the steroid binding site of rat liver 3α-HSD. A stereoview of the binding pocket of rat 3α-HSD containing the cofactor $NADP^+$ and the competitive inhibitor testosterone. The catalytic residues are colored red (Tyr55 and His117). The remaining residues are Thr24, Leu54, Phe118, Phe129, Thr226, Trp227, Asn306, and Tyr310.

steroid-binding pocket of rat liver 3α-HSD (EC 1.1.1.213, AKR1C9).[2] We have exploited the known crystal structure of the E·$NADP^+$·testosterone (*8*) ternary complex to conduct this analysis.

The highly positional and stereoselective enzyme rat 3α-HSD catalyzes the NAD(P)(H)-linked interconversion of 3-ketosteroid substrates and 3α-hydroxysteroids (*9*). It is involved in the inactivation of steroid hormones that include androgens, progestins, and glucocorticoids. In endocrine target tissues, 3α-HSD isoforms convert 5α-dihydrotestosterone (a potent androgen with a K_d of 10^{-11} M for the androgen receptor) into 3α-androstanediol (a weak androgen with a K_d of 10^{-6} M for the androgen receptor) (*10*, *11*). In the central nervous system (CNS), 3α-HSD isoforms are implicated in the conversion of 5α-dihydroprogesterone to allopregnanolone, an allosteric effector of the $GABA_A$ receptor (*12*−*14*). Thus, 3α-HSD isoforms can regulate the ligand occupancy of nuclear receptors and membrane-bound ion channels (*15*−*18*). Unlike the rat enzyme, the human homologues of 3α-HSD (AKR1C1−AKR1C4) display functional plasticity in that these isoforms demonstrate 3α-, 17β-, and/or 20α-HSD activities in different ratios with significantly decreased k_{cat} values (*19*). The high levels of sequence identity of the rat and human enzymes raise the issues of what governs steroid hormone affinity and what determines k_{cat}. Because rat liver 3α-HSD is the most thoroughly characterized steroid hormone-transforming AKR, it provides a solid model for tackling these problems, not just within the rubric of aldo-keto reductases, but may also provide some insight into other steroid-transforming enzymes as well.

The three-dimensional structures of the apoprotein, the E·$NADP^+$ binary complex, and the E·$NADP^+$·testosterone ternary complex have been determined for rat 3α-HSD (*8*, *20*−*21*). The protein adopts an $(\alpha/\beta)_8$-barrel fold or TIM barrel motif of alternating α helices and β strands. The steroid binding site is formed by a cylindrical cavity comprised of loops on the C-terminal side of the protein. A comparison of the binary and ternary complexes indicates loop movement upon steroid binding, and the loops that undergo the greatest conformational change are the β1−α1 loop, loop B, and loop C. Within these loops, 10 residues comprise the steroid-binding pocket of 3α-HSD. Two are catalytic, Y55 and H117 (*22*), and the remainder are T24, L54, F118, F129, T224, W227, N306, and Y310 (Figure 1). An alignment of the putative steroid binding site residues of AKR1C enzymes shows that while there is variability, a few discrete residues are highly conserved (*23*). For example, T226 in rat 3α-HSD is not at all conserved among any of the AKR1C human isoforms. Conversely, both F118 and W227 are highly conserved, and these residues probably play more important structural and/or functional roles.

Here we present the first systematic analysis of contact residues in a steroid binding site based on the available X-ray structure of a complete protein. We found that the alanine mutants did not alter the K_d for cofactor (first ligand). The K_d for the binding of testosterone and progesterone to the

[2] The nomenclature for the AKR superfamily was recommended at the 8th International Symposium on Enzymology and Molecular Biology of Carbonyl Metabolism. The following website provides updated information on the AKR superfamily: http://www.med.upenn.edu/akr.

Table 1: Oligonucleotide Primers Used To Generate Alanine Mutations in Rat Liver 3α-HSD[a]

mutant	primer
T24A	forward, 5′-dGGGTTTGGAACCGCTGTGCCTGAGAAGG-3′
	reverse, 5′-dCCTTCTCAGGCACAGCGGTTCCAAACCC-3′
L54A	forward, 5′-GACTCTGCTTATGCGTACGAAGTAGAAGAG-3′
	reverse, 5′-CTCTTCTACTTCGTACGCATAAGCAGAGTC-3′
F118A	forward, 5′-GTGGATCTTTATATTATTCATGCCCCAATGGCTTTGCAG-3′
	reverse, 5′-CTGCAAAGCCATTGGGGCATGAATAATATAAAGATCCAC-3′
F129A	forward, 5′-GGAGATATATTTGCCCCACGAGATGAG-3′
	reverse, 5′-CTCATCTCGTGGGGCAAATATATCTCC-3′
T226A	forward, 5′-GGAAGTTCACGAGACAAAGCATGGGTGGATCAGAAAAGTCC-3′
	reverse, 5′-GGACTTTTCTGATCCACCCATGCTTTGTCTCGTGAACTTCC-3′
W227A	forward, 5′-GGAAGTTCACGAGACAAAACAGCGGTGGATCAGAAAAGTCC-3′
	reverse, 5′-GGACTTTTCTGATCCACCGCTGTTTTGTCTCGTGAACTTCC-3′
N306A	forward, 5′-CAGAAATTTCAGATACGCCAATGCAAAATATTTTGATGACCATCC-3′
	reverse, 5′-GGATGGTCATCAAAATATTTTGCATTGGCGTATCTGAAATTTCTG-3′
Y310A	forward, 5′-CAGATACAACAATGCAAAAGCCTTTGATGACCATCCCAATCATCC-3′
	reverse, 5′-GGATGATTGGGATGGTCATCAAAGGCTTTTGCATTGTTGTAT CTG-3′

[a] Underlined codons indicate the site of the mutation.

E·NADPH complex was more adversely affected when alanine replaced a hydrophobic residue. The largest effects were on k_{cat}/K_m and were reflected by dramatic decreases in k_{cat}, suggesting that the mutations severely affected the rate-determining step in the 3α-HSD-catalyzed reaction. Transient kinetic analyses showed that alanine mutations of aromatic hydrophobic residues altered the rate-determining step. Whereas product release in the wild-type (WT) protein was the largest determinant of k_{cat} for 3α-hydroxy-5α-androstan-17-one (androsterone) oxidation, chemistry became rate-limiting when hydrophobic residues were mutated to alanine. This suggests that binding cavity residues not only control steroid hormone affinity but also affect the rate of oxidation, which becomes rate-limiting when the steroid fails to make proper contact with these residues.

EXPERIMENTAL PROCEDURES

Materials. The primers used for site-directed mutagenesis were purchased from GibcoBRL. The pET-16b expression vector was purchased from Novagen. J. E. Walker of the MRC Laboratory of Molecular Biology (Cambridge, U.K.) kindly provided the *Escherichia coli* C41 (*DE3*) strain. The Quikchange site-directed mutagenesis kit was purchased from Stratagene. NAD^+, $NADP^+$, and NADPH were purchased from Roche Biochemicals. All steroids were obtained from Steraloids. All other compounds were obtained from Sigma or Aldrich and were ACS grade or better.

Mutagenesis, Expression, and Purification of Recombinant WT and Mutant 3α-HSDs. The pET16b-3α-HSD expression vector and details of the site-directed mutagenesis protocols have been described previously (*24*). The forward and reverse primers used to produce the T24A, L54A, F118A, F129A, T226A, W227A, N306A, and Y310A mutants are listed in Table 1. Dideoxy sequencing ensured the fidelity of the mutant constructs. The pET16b-3α-HSD vectors encoding each of the mutants were used to transform *E. coli* C41 (*DE3*) cells. The overexpressed proteins were purified by successive chromatography on DE-52 cellulose and Sepharose Blue as described previously (*25*). The T24A mutant was purified in a single step with a DE-52 anion exchange column followed by elution with a NaCl gradient (from 10 to 250 mM NaCl). SDS−PAGE was utilized to assess protein purity, and protein concentrations were determined by the method of Lowry (*26*) using bovine serum albumin as a standard.

The homogeneous WT and mutant enzymes were stored at −80 °C in storage buffer [20 mM potassium phosphate (pH 7.0) with 30% glycerol, 1 mM EDTA, and 1 mM β-mercaptoethanol]. Specific activity measurements were made using standard assay conditions consisting of 100 mM potassium phosphate buffer (pH 7.0), 2.3 mM NAD^+, and 75 μM androsterone with 4% acetonitrile as a cosolvent. For kinetic measurements, each batch of enzyme was analyzed in the standard androsterone assay. The same number of units based on the final specific activity of that mutant was then added to each assay.

Determination of K_d Values for NADPH by Fluorescence Titration. K_d values for the binding of cofactor NADPH to r3α-HSD and its mutants were determined by measuring protein fluorescence on an AVIV automated titrating differential/ratio spectrofluorimeter following the incremental addition of NADPH (40 nM to 6.0 μM). Each sample contained 0.20 μM protein in 10 mM potassium phosphate buffer (pH 7.0) containing 1 mM EDTA at 25 °C. The total volume change from the addition of cofactor was less than 2%. The samples were excited at 290 nm with the fluorescence emission scanned from 305 to 480 nm with the excitation and emission band-pass set at 5 nm. Since the enzymes bind NADPH very tightly, the depletion of ligand during the titration was taken into account using a modified Scatchard analysis as described by Ehrig (*27*). Briefly, the fractional saturation (α) by ligand of the total available ligand binding sites was equated to the ratio of $\Delta F/\Delta F_{max}$, where ΔF is the change in fluorescence at a given ligand concentration and ΔF_{max} is the maximal change in fluorescence at a fully saturating ligand concentration. The dissociation constant was determined using eq 1, where the fractional saturation (α) is related to the total concentration of ligand (L_0).

$$L_0/\alpha = K_d/(1-\alpha) + E_0 \quad (1)$$

where E_0 is the total active site concentration and K_d is the dissociation constant. The K_d was obtained from the slope of a plot of $1/(1-\alpha)$ versus L_0/α, where the *y*-axis intercept yields the concentration of binding sites (*28*). The value of K_{dNADPH} for the WT enzyme was 137 ± 12 nM and was

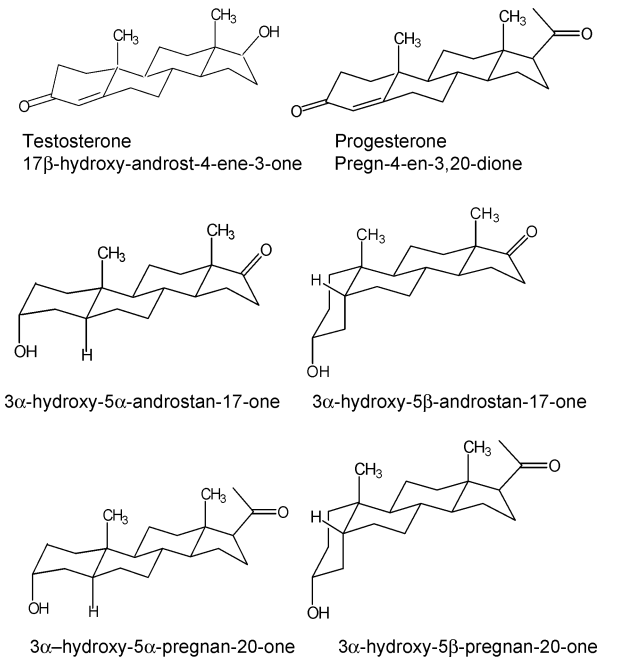

FIGURE 2: Steroid hormones (competitive inhibitors) and substrates used to analyze rat liver 3α-HSD and its alanine mutants. Most hydrogens have been eliminated for clarity.

similar to previously reported values of K_{dNADPH} (140 nM) when fluorescence data were fit to a straight hyperbola (*24*).

Determination of K_d Values for Testosterone and Progesterone by Fluorescence Titration. K_d values for the binding of testosterone and progesterone (Figure 2) to 3α-HSD and its mutants were determined by titrating the energy transfer band of the E•NADPH binary complex by the incremental addition of testosterone (100 nM to 120 μM) and progesterone (10 nM to 75 μM). Each sample contained 0.20 μM enzyme, 10 mM potassium phosphate buffer (pH 7.0) containing 1 mM EDTA, 4% acetonitrile, and 4.0 μM NADPH at 25 °C. On the basis of the K_{dNADPH} for each alanine mutant (120−340 nM), each enzyme sample was completely saturated with the cofactor. The samples were excited at 290 nm with fluorescence emission monitored from 305 to 480 nm with the excitation and emission band-pass set at 5 nm. The emission signal at λ_{max} (435 nm) was used to determine K_d values. A modified Scatchard analysis identical to that described above was utilized to determine the K_d values for testosterone and progesterone.

Determination of Steady-State Kinetic Parameters. Initial velocities were measured on a Beckman DU-640 UV−vis spectrophotometer by observing the rate of change in absorbance of the pyridine nucleotide at 340 nm ($\epsilon = 6270$ M^{-1} cm^{-1}) in 1 mL samples using a path length of 1 cm. Measurements of the K_m and k_{cat} values for the oxidation of androsterone, 3α-hydroxy-5β-androstan-17-one, 3α-hydroxy-5α-pregnan-20-one, and 3α-hydroxy-5β-pregnan-20-one (Figure 2) were made in 100 mM potassium phosphate buffer (pH 7.0) containing 2.3 mM $NAD(P)^+$ with 6% acetonitrile as a cosolvent at 37 °C. To compare steady-state kinetic parameters with transient kinetic results, androsterone oxidation by the WT, W227A, F118A, and T226A mutants was also monitored in 10 mM potassium phosphate buffer (pH 7.0) with 4% acetonitrile at 25 °C.

To increase the sensitivity of the assay, a spectrofluorimetric assay was employed when necessary using either an AVIV automated titrating differential/ratio spectrofluorimeter or a Hitachi F-2500 fluorescence spectrophotometer. Samples (0.5 or 1.0 mL) containing the same final concentrations as described for the UV−vis spectrophotometer assays were used. Excitation and emission wavelengths were set at 340 and 450 nm, respectively, and the rate of change in fluorescence emission of the cofactor at 450 nm was monitored to determine initial velocities. Changes in fluorescence units were converted to nanomoles of cofactor by using standard curves of fluorescence emission at 450 nm versus known cofactor concentrations. Standard curves were constructed on a daily basis.

All reactions were initiated by the addition of enzyme and were corrected for nonenzymatic rates. All k_{cat} and K_m values were calculated using GRAFIT 5.0 (Erithacus Software) by fitting untransformed data with a hyperbolic function, as originally described by Wilkinson (*29*), yielding estimates of the kinetic constants and their associated standard errors.

Transient Kinetics. Transient kinetic traces were acquired using an Applied Photophysics SX-18MV-R stopped-flow apparatus in fluorescence mode with excitation at 340 nm and emission monitored using a 450 nm band-pass filter. For these measurements, the temperature was set at 25 °C and not 37 °C to slow the pre-steady-state rates for more manageable data acquisition. Reactions were carried out in 10 mM potassium phosphate buffer (pH 7.0) and 4% acetonitrile. Standard curves with known NADPH concentrations were constructed on a daily basis. The change in signal was monitored as a function of time for the $NADP^+$-dependent oxidation of androsterone. For single-turnover experiments, one syringe contained 2 μM enzyme and limiting $NADP^+$ (1.0 μM) while the second syringe contained increasing concentrations of androsterone (final concentration range of 2−45 μM). For multiple-turnover experiments, one syringe contained 1.8−2.0 μM enzyme and excess $NADP^+$ (60 μM) while the second syringe contained increasing concentrations of androsterone (final concentration range of 5−45 μM).

The progress curves were analyzed using the SX18.MV-R software version 4.46. Progress curves from single-turnover experiments fitted a first-order process. Since a plot of k_{obs} versus steroid concentration showed saturation kinetics, rates were fitted to eq 2 to determine k_{lim} values.

$$k_{obs} = k_{max}[\text{steroid}]/(K_{0.5} + [\text{steroid}]) \qquad (2)$$

where $k_{lim} = k_{max}$ for single turnover and $k_{max} = k_{max}$ for multiple turnovers. In multiple-turnover experiments showing burst phase kinetics, the rate constants for the burst phase (k_{burst}) and the rate constants for the linear phase of the reaction (k_{ss}) displayed saturation kinetics. Data were fit to eq 2 to determine the k_{max} for the burst phase and the k_{max} for the steady-state rate. In multiple-turnover experiments showing no burst phase, the rate constants for the linear phase were fit to eq 2 to determine the k_{max} for the steady-state rate.

RESULTS

Expression and Purification of Recombinant WT and Mutant 3α-HSDs. WT 3α-HSD and alanine mutants of the residues that line the testosterone binding pocket, e.g., T24A, L54A, F118A, F129A, T226A, W227A, N306A, and Y310A,

Table 2: Determination of K_d Values for Binding of Ligand to Rat 3α-HSD and Its Alanine Mutants[a]

enzyme	K_d(NADPH) (nM)	K_d(testosterone) (μM)	K_d(progesterone) (μM)
WT	137 ± 12	2.54 ± 0.22	0.285 ± 0.22
T24A	255 ± 17	2.12 ± 0.19	0.579 ± 0.58
L54A	231 ± 22	7.24 ± 0.79	1.85 ± 0.19
F118A	341 ± 26	6.68 ± 0.71	1.84 ± 0.20
F129A	120 ± 8	4.30 ± 0.44	1.41 ± 0.13
T226A	279 ± 15	0.99 ± 0.10	0.211 ± 0.22
W227A	244 ± 20	10.7 ± 1.2	6.49 ± 0.69
N306A	207 ± 18	6.67 ± 0.77	1.93 ± 0.18
Y310A	249 ± 19	9.20 ± 0.94	2.19 ± 0.19

[a] These values are revised from previously published analyses (*37*). The current data set utilizes a broader dynamic range of ligand concentrations. In addition, ternary complex formation was assessed under conditions in which the enzyme was present wholly as E·NADPH and all binding constants were computed using a modified Scatchard analyses (*27*). These values supersede the earlier ones.

were overexpressed in *E. coli* C41 (*DE3*) cells and purified to homogeneity. The specific activities of the purified proteins for the NAD^+-dependent oxidation of androsterone were 1.60, 0.86, 0.08, 0.01, 0.03, 0.96, 0.006, 0.09, and 0.10 μmol min^{-1} mg^{-1} for the WT enzyme and the T24A, L54A, F118A, F129A, T226A, W227A, N306A, and Y310A mutants, respectively. The WT and mutant forms of 3α-HSD appeared as single homogeneous bands with the same molecular mass on SDS−PAGE gels (data not shown).

Determination of the Binding Constants for NADPH. To determine whether the alanine mutations affected binding of the cofactor to rat 3α-HSD, we assessed the ability of NADPH to quench the intrinsic tryptophan fluorescence in each mutant. This study is possible because 3α-HSD catalyzes an ordered bi-bi kinetic mechanism in which there is an obligatory requirement for cofactor to bind before steroid hormone (*30*−*33*). Each mutant had the same relative intrinsic tryptophan fluorescence except for W227A, which had ∼65% of the intrinsic tryptophan fluorescence of the WT enzyme. Rat 3α-HSD has three tryptophans, and previous mutation of these residues indicated that W227 contributed to 33% of the fluorescence signal (*25*). Fluorescence titration of each alanine mutant with NADPH showed only minor changes in K_d of 2−3-fold for the cofactor (Table 2) and cannot account for the 100-fold variation in the specific activity of the mutants. Because the binding of the cofactor requires interactions with 21 different residues (*34*), we conclude that the alanine mutations had not affected the cofactor affinity of this site.

Determination of the Binding Constants for Testosterone and Progesterone. To determine whether the alanine mutations affected binding of the steroid hormone to the 3α-HSD·NADPH binary complex, we devised a novel assay. For this assay, we exploited the observation that the energy transfer band produced during the formation of the E·NADPH binary complex could be quenched by steroid hormone. This phenomenon can be explained by the steroid inserting itself between W86 and the nicotinamide ring of the cofactor, thereby disrupting the energy transfer (*25*). By adding steroid incrementally to the E·NADPH complex, we showed that the energy transfer band could be titrated to give a binding isotherm and a K_d value similar to that observed in equilibrium dialysis. Previous estimates of K_d values for the binding of testosterone to the 3α-HSD·NADPH binary complex have relied on the technically more difficult microequilibrium dialysis assay using radiolabeled testosterone. For these experiments, NADH instead of NADPH was utilized because of the instability of the NADPH cofactor for overnight dialysis (*25*). The K_d value for testosterone binding by equilibrium dialysis was found to be 4.2 ± 0.8, and the K_d value for testostorone binding by fluorimetric methods was found to be 2.54 ± 0.28 μM. The ability of NADPH to increase steroid affinity has been previously noted (*9*). Using this new assay, we were able to efficiently determine K_d values for testosterone and progesterone for the WT and each of the alanine mutants (Table 2).

Results showed that steroid hormone binding was affected by alanine mutations resulting in K_d changes of up to 23-fold. Alanine mutations of short polar groups such as T24A and T226A gave K_d values for testosterone and progesterone similar to those observed for the WT enzyme. The largest adverse effects were obtained when alanine replaced aromatic residues. The W227A mutant displayed the lowest affinity for both testosterone and progesterone among all the mutant enzymes. Testosterone binding affinity decreased by 4-fold in the W227A mutant, and progesterone binding affinity decreased by 23-fold compared to the WT value.

Effects of the Alanine Mutations on Substrate Turnover. Rat 3α-HSD will reduce 3-ketosteroids and oxidize 3α-hydroxysteroids of C_{19} and C_{21} steroids irrespective of whether they contain A/B *trans* or A/B *cis* ring fusions. The latter ring fusion distorts the A ring 90° out of plane. To determine whether the alanine mutants would discriminate among these steroids, 3α-hydroxysteroids of these configurations were screened as substrates (Figure 2). Measurements of catalytic efficiency (k_{cat}/K_m) showed that in some instances profound changes of more than 2 log units had occurred as a result of the alanine mutations (see the Supporting Information). Substitution of short polar groups such as T24A and T226A led to k_{cat}/K_m values indistinguishable from that of the WT enzyme, while substitution of aromatic hydrophobic residues (W227A, F129A, and F118A) gave the largest decreases in k_{cat}/K_m. The effects on k_{cat}/K_m followed the same rank order for C_{19} steroids irrespective of the A/B ring configuration. We predict that the outcome is the same for C_{21} steroids, but the data are incomplete because of constraints imposed by steroid solubility.

The effects on k_{cat}/K_m were dissected by examining the effects of the alanine mutations on k_{cat} and K_m individually. Overall, the effects on K_m were small (with the largest increase being only 10-fold from the WT value) and were less profound than the effects on K_d values for steroid hormones. By far, the largest effects were on k_{cat}, where changes of almost 300-fold were observed for some mutant proteins. Globally, alanine mutants affected k_{cat} in the same rank order as the effects on k_{cat}/K_m, showing that the dominant effect was on k_{cat}.

To determine if the effects on k_{cat}/K_m were cofactor-dependent, steady-state kinetic parameters for the substrate pair $NADP^+$ and androsterone were also determined. Results showed an essentially similar pattern whereby changes in K_m values were small in comparison to changes in k_{cat} values. The most dramatic decreases were observed for alanine mutations of large hydrophobic residues. For example, the W227A mutant showed a decrease in k_{cat} of more than 200-fold, but only showed an increase in K_m of ∼4-fold.

Table 3: Comparison of k_{cat} Values with the Microscopic Rate Constants Detected in the Transient State for the Oxidation of Androsterone and $NADP^+$

enzyme	k_{cat} in the steady state[a] (s^{-1})	k_{lim} of single turnover[a] (s^{-1})	k_{max} of the burst in multiple turnovers[a] (s^{-1})	k_{max} of the steady state in multiple turnovers[a] (s^{-1})
WT	0.83	68	51	0.77
T226A	0.57	98	110	0.67
F118A	0.0083	0.0067	none	0.0075
W227A	0.0053	0.0052	none	0.0063

[a] Steady-state and transient-state determinations were performed at 25 °C with 10 mM potassium phosphate buffer (pH 7.0) and 4% acetonitrile.

Similarly, the F118A and F129A mutants decreased k_{cat} more than 100-fold but increased K_m by a modest 2-fold (see the Supporting Information).

Effects of the Alanine Mutations on Transient Kinetics of Steroid Turnover. Single-turnover and multiple-turnover experiments were performed on the WT, W227A, F118A, and T226A enzymes to determine the roles of mutated residues on the microscopic rate constants for steroid turnover (Table 3 and Figures 3 and 4). W227A and F118A were chosen since their k_{cat} values were maximally depressed. As a comparison, transient-state kinetic analyses were performed on T226A because it exhibited steady-state kinetic parameters similar to those of the WT enzyme. The substrates used in these reactions were $NADP^+$ and androsterone.

Using the WT enzyme, single-turnover experiments were performed under conditions in which the enzyme could not recycle. As the androsterone concentration increased, the k_{obs} for the kinetic transients exhibited saturation kinetics (Figure 3A,B) in which k_{lim} values (68 s^{-1}) were much greater than k_{cat} values (0.83 s^{-1}). Under multiple-turnover conditions, the oxidation of androsterone exhibited burst kinetics (Figure 4A). The amplitude of the burst coincided with the concentration of enzyme added (>98% of the protein), and the k_{max} of the burst (51 s^{-1}) coincided with the k_{lim} values observed in the single-turnover experiments. In contrast, the k_{max} (0.77 s^{-1}) for the steady-state turnover of androsterone was identical to k_{cat} (0.83 s^{-1}). This suggests that the slow release of products is partially rate-determining for the WT enzyme when $NADP^+$ and androsterone are cosubstrates.

When W227A and F118A enzymes were used in single-turnover experiments for androsterone oxidation, saturation kinetics were observed (Figure 3C,D), but their k_{lim} values (0.0052 and 0.0067 s^{-1}, respectively) were essentially identical to their k_{cat} values (0.0053 and 0.0083 s^{-1}, respectively). Under multiple-turnover conditions, the oxidation of androsterone catalyzed by these same mutants no longer showed a burst phase (Figure 4C,D). Saturation kinetics were again observed, and k_{max} equaled k_{cat}. This suggests that the slow release of products is no longer rate-limiting since another event has become the slowest overall. Conversely, the T226A mutant exhibited transient-state kinetic parameters similar to those of the WT protein, whereby k_{lim} (98 s^{-1}) is greater than k_{cat} (0.57 s^{-1}) in single-turnover experiments (Figure 3E,F). Under multiple-turnover conditions, the oxidation of androsterone was similar to that observed with the WT protein in that burst phase kinetics were observed (k_{max} of burst = 110 s^{-1}) and coincided with the k_{lim} for the single-turnover experiments (Figure 4E,F). Again, the k_{max} (0.67 s^{-1}) for steady-state turnover was identical to k_{cat} (0.57 s^{-1}).

DISCUSSION

We systematically dissected the role of individual amino acid residues implicated in the binding of testosterone to rat 3α-HSD, a representative AKR. We used alanine scanning mutagenesis and found that the residues in the pocket dictate the correct positioning of steroid substrates to facilitate catalysis as shown by large decreases in k_{cat} values of more than 2 log units. Furthermore, these same residues can influence the rate-determining step as revealed by microscopic rate constants determined by transient kinetics. In contrast, the largest effects on steroid hormone binding (K_d) were highlighted by a more modest 23-fold change.

To ensure that the mutations did not disrupt cofactor binding, quenching of the intrinsic protein fluorescence upon NADPH binding showed that cofactor affinity was essentially unaltered. Mutation of the steroid-binding pocket residues into alanine produced only marginal changes in the K_d values for NADPH, where each mutant bound cofactor with nanomolar affinity.

We used a novel fluorescence quench assay to assess the binding of testosterone and progesterone to rat 3α-HSD. Here the ability of the steroid hormone to quench the energy transfer band in the E·NADPH binary complex was exploited. It was found that the largest effects on K_d were a 4-fold increase for testosterone binding and a 23-fold increase for progesterone binding. Substitution of alanine for short polar residues produced only minor changes, whereas the more pronounced effects were seen when alanine replaced aromatic hydrophobic residues. Both ligands were bound by the mutants in a similar rank order, where the W227A mutant most adversely affected steroid hormone binding. At first glance, it is unclear why the W227A mutant decreased the affinity for progesterone by 23-fold but decreased the affinity for testosterone by only 4-fold. In the E·$NADP^+$·testosterone crystal structure, W227 interacts with the A and B rings of the steroid (*8*) and not with the side chain at C17, which is where the difference in the structure of the two hormones exists. However, W227 may adopt different conformations, which is evident when the crystal structures of rat 3α-HSD (AKR1C9) and human type 3 3α-HSD (AKR1C2) (23) are compared. In the AKR1C2·$NADP^+$·ursodeoxycholate ternary complex, W227 rotates 120° relative to its position in the AKR1C9·$NADP^+$·testosterone ternary complex. In the former structure, ursodeoxycholate is now bound essentially backward (A ring in the D ring position) and upside down (α-face inverted) relative to the position of testosterone in rat 3α-HSD. Thus, rotation of W227 in the human type 3 3α-HSD permits a C24 steroid to bind in a new orientation by contacting the C and D rings of ursodeoxycholate and preventing clashing with the C18 angular methyl group. The absence of W227 in the W227A mutant may now permit an alternative binding mode for the C21 steroid progesterone, thereby decreasing the affinity for this ligand.

The unexpected finding in this study was the profound effects of the alanine mutations on k_{cat}/K_m that were largely reflected in k_{cat}. Identical trends were observed irrespective of whether the NAD^+- or $NADP^+$-dependent oxidation of

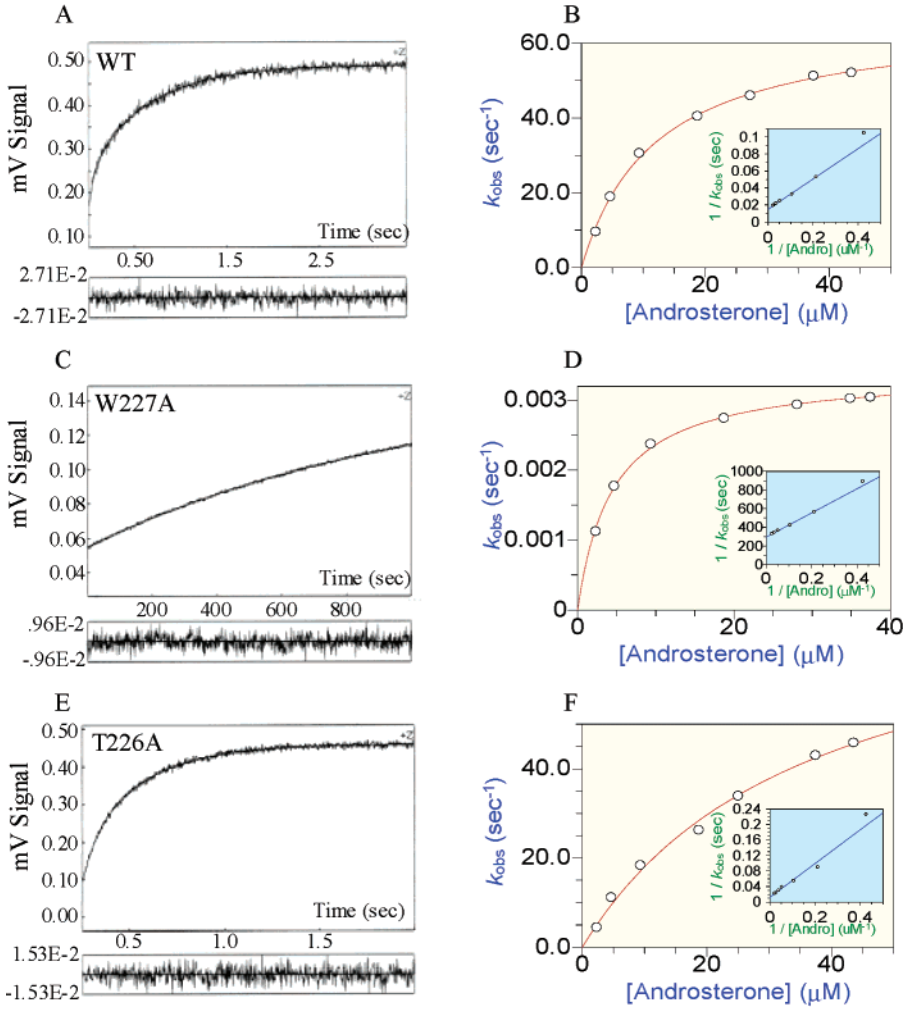

FIGURE 3: Representative transient kinetic traces for the NADP$^+$-dependent oxidation of androsterone by WT, W227A, and T226A proteins under single-turnover conditions. Panels A, C, and E depict the average from five traces of single-turnover stopped-flow progress curves in the fluorescence mode with excitation at 340 nm and emission monitored using a 450 nm band-pass filter. Reactions were performed in 10 mM phosphate buffer (pH 7.0) at 25 °C and 4% acetonitrile. The transient trace in panel A was the result of mixing 2 μM WT enzyme and 1 μM NADP$^+$ in syringe 1 and 18.8 μM androsterone in syringe 2. The transient trace in panel C was the result of mixing 2 μM W227A enzyme and 1 μM NADP$^+$ in syringe 1 and 6 μM androsterone in syringe 2. The transient trace in panel E was the result of mixing 2 μM T226A enzyme and 1 μM NADP$^+$ in syringe 1 and 18.8 μM androsterone in syringe 2. First-order rate constants (k_{obs}) were determined by fitting data to a single-exponential equation over a range of androsterone concentrations (3−45 μM). The bottom traces in each panel show a plot of residuals from the single-exponential fit. Panels B, D, and F are plots of k_{obs} versus androsterone concentration for WT, W227A, and T226A enzymes, respectively, which exhibit saturation kinetics.

androsterone was assessed. k_{cat} represents the rate-limiting step in the reaction, raising the issue of why the alanine mutants affect this step. 3α-HSD catalyzes an ordered bi-bi kinetic mechanism in which the cofactor binds first and leaves last (*30*−*33*). Studies on aldose reductase (AKR1B1), another representative AKR, indicated that the rate-determining step in the reduction direction was governed by the slow isomerization of a tight E*·NADP$^+$ complex to a loose E·NADP$^+$ complex, defined by k_4, which governs the rate of NADP$^+$ release (eq 3) (*35*). The slow release of NADP$^+$ was supported by burst kinetics.

$$\text{E} + \text{NADH(H)} \underset{k_2}{\overset{k_1}{\rightleftharpoons}} \text{E·NADP(H)} \underset{k_4}{\overset{k_3}{\rightleftharpoons}} \text{E*·NADP(H)} \quad (3)$$

In the oxidation direction, no burst of NADPH production was observed since chemistry was greatly rate-limiting overall by 85% and k_4 was a minor contributor to the overall reaction (15%). On the basis of these previous findings from a related AKR, we hypothesized that the rate-determining step in the oxidation of 3α-hydroxysteroids by AKR1C9 would be chemistry. Therefore, we expected no burst of NADPH production under multiple-turnover conditions.

We have previously conducted a stopped-flow fluorescence kinetic study, in which we determined k_4 for the release of NADP(H) predicted by a two-step binding model (*24*). In each case, this microscopic rate constant was larger than k_{cat}. We have re-examined the microscopic events associated with cofactor binding using a more sensitive stopped-flow instrument with less dead time and superior data fitting software (*36*). While both studies support a slow conformational change upon NADP(H) binding, the latter study provides evidence for a three-step binding model (eq 4).

$$\text{E} + \text{NADH(H)} \underset{k_2}{\overset{k_1}{\rightleftharpoons}} \text{E·NADP(H)} \underset{k_4}{\overset{k_3}{\rightleftharpoons}} \text{E*·NADP(H)} \underset{k_6}{\overset{k_5}{\rightleftharpoons}} \text{E**·NADP(H)} \quad (4)$$

Kinetic transients of NADP(H) binding best fitted a biex-

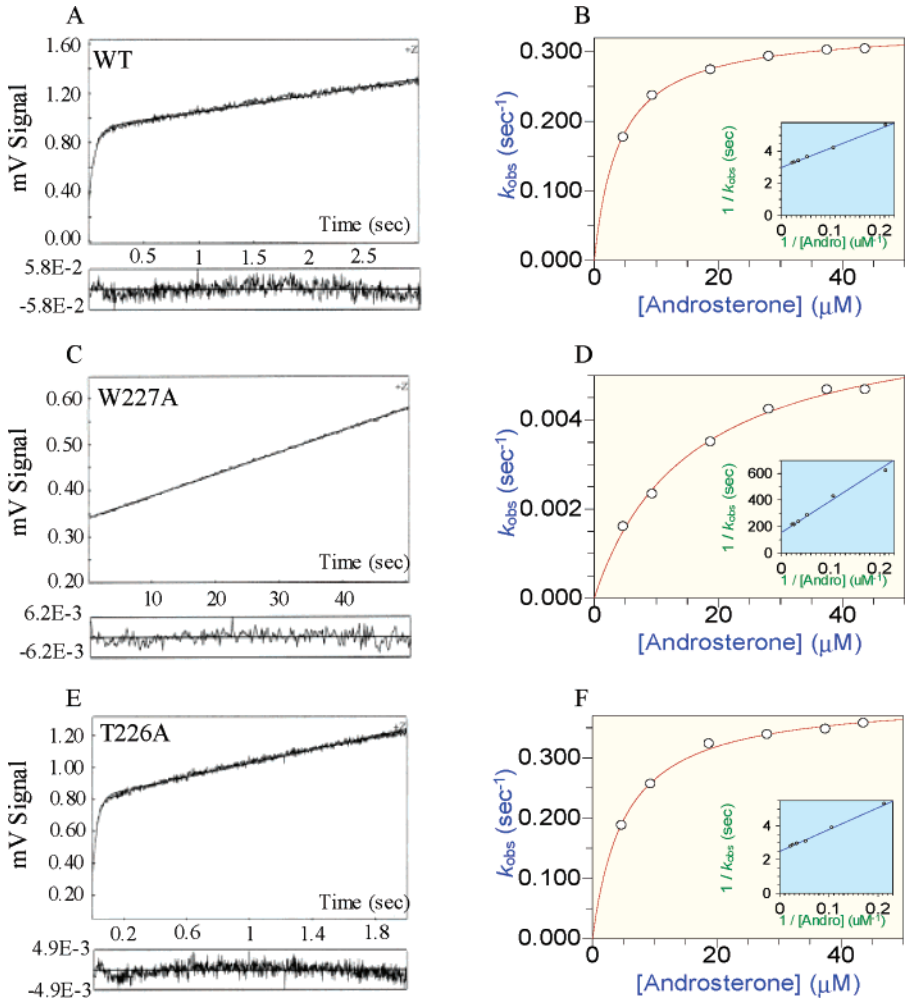

FIGURE 4: Representative transient kinetic traces for the NADP$^+$-dependent oxidation of androsterone by WT, W227A, and T226A proteins under multiple-turnover conditions. Panels A, C, and E depict the average from five traces of multiple-turnover stopped-flow progress curves in the fluorescence mode with excitation at 340 nm and emission monitored using a 450 nm band-pass filter. Reactions were performed in 10 mM phosphate buffer (pH 7.0) at 25 °C and 4% acetonitrile. The transient trace in panel A was the result of mixing 2 μM WT enzyme and 60 μM NADP$^+$ in syringe 1 and 37.6 μM androsterone in syringe 2. The transient trace in panel C was the result of mixing 2 μM W227A enzyme and 60 μM NADP$^+$ in syringe 1 and 56.2 μM androsterone in syringe 2. The transient trace in panel E was the result of mixing 1.8 μM T226A enzyme and 60 μM NADP$^+$ in syringe 1 and 75 μM androsterone in syringe 2. Progress curves shown in panels A and E emphasize the pre-steady-state burst. For the WT and T226A enzymes, first-order rate constants for the burst phase (k_{burst}) and the zero-order rate constants for the steady state (k_{ss}) were obtained by fitting data to the equation for a single exponential with a steady state ($y = Ae^{-k_{burst}t} + k_{ss}t + C$, where y is the signal, A the amplitude of the burst, t the time, and C the intercept) over a range of androsterone concentrations (5−45 μM). For the W227A enzyme, zero-order rate constants for the steady state were obtained by fitting data to the linear regression equation ($y = k_{ss}t + C$, where y is the signal, t the time, and C the intercept) over a range of androsterone concentrations. Panels B, D, and F are plots of k_{ss} vs androsterone concentration for WT, W227A, and T226A enzymes, respectively, which exhibit saturation kinetics for the linear, steady-state phase of the reaction.

ponential process comprised of a fast phase and a slow phase, in which the microscopic rate of the slow phase of NADPH release now approaches the value of k_{cat} (Y. Jin and T. M. Penning, unpublished results). Thus, in the enzymatic oxidation of androsterone using NADP$^+$ as a cofactor, product release (NADPH) could be partially rate-limiting.

This study shows that while k_{cat} decreased by up to 2 log units in the alanine mutants, K_{dNADPH} is essentially unchanged which suggests that the k_{off}/k_{on} rates for the mutants were unaltered. If changes in the binding and/or release of steroid were responsible for the large decrease in k_{cat}, then this should be reflected by large changes in K_d for the competitive inhibitors, testosterone and progesterone. However, profound changes in these values were not observed. We therefore hypothesized that the alanine mutants that dramatically decreased k_{cat} must adversely affect either the hydride transfer or proton donation events that occur in the chemical step. Our hypothesis must explain why alanine mutations of short polar residues retained k_{cat}/K_m values similar to that of the WT enzyme and why alanine mutations of hydrophobic aromatic residues gave the largest deviations in k_{cat}/K_m.

To test our hypothesis, we conducted single-turnover and multiple-turnover transient kinetics for the oxidation of androsterone catalyzed by the WT enzyme and compared these values with those of W227A and F118A, the mutants with the most depressed k_{cat} values. W227 and F118 are also highly conserved residues among AKR1C isoforms. We also performed experiments on T226A, a mutant that exhibited k_{cat} values similar to that of the WT. T226 is not conserved among AKR1C enzymes. Thus, the mutations we used for our transient kinetic work were chosen on the basis of their kinetic profile (mutants with a very low k_{cat} vs mutants with

a high k_{cat}) and the fact that they were not catalytic residues. Other alanine mutants exhibited intermediary decreases in k_{cat}/K_m values, but these residues might still play an important function in steroid binding and catalysis. For example, the L54A mutant decreased k_{cat} by 30-fold and is predicted to play a significant role in steroid positioning. AKR1C1 and AKR1C2 differ by only seven amino acid residues, of which only one is located in the steroid-binding pocket. (AKR1C1 has a leucine at residue 54, but AKR1C2 has a valine at this same position.) However, AKR1C1 has high 20α-HSD activity, while AKR1C2 has no detectable 20α-HSD activity but has a very high affinity for bile acids (*19*, *23*).

Single-turnover experiments were designed so that the enzyme could not recycle. After mixing, the events that were monitored include steroid binding, chemistry, and product release. However, no lag phase kinetics are observed upon mixing the steroid, suggesting that the binding of the second substrate is not a slow event. Thus, the events monitored under single-turnover conditions are based only on the rate of steroid transformation and product release. A single turnover of androsterone oxidation by WT showed that k_{lim} is considerably greater than k_{cat}, which indicates that chemistry is not rate-limiting. Multiple turnovers of androsterone oxidation exhibited burst phase kinetics, which confirms that a subsequent step after steroid transformation, specifically product release, is rate-limiting overall.

Unlike AKR1B1 in which chemistry was rate-limiting in the oxidation of xylitol, our study shows that the rate-determining step for the oxidation of androsterone by AKR1C9 is governed by product release. Interestingly, AKR1B1 undergoes a two-step binding mechanism for NADP(H), which involves the formation of a safety belt across the pyrophosphate bridge, resulting in an overall increase in cofactor affinity of 650-fold in the tight complex (*35*). In contrast, AKR1C9 undergoes a three-step binding mechanism for NADP(H) (*36*), which involves the formation of a cofactor anchor between R276 and the 2′-phosphate of AMP but not the formation of a safety belt (*24*). The final step is the slowest, but the overall increase in affinity for the cofactor achieved in this binding mechanism of 30-fold is smaller than that for AKR1B1. Thus, enzymes from the same family with a high level of sequence identity differ in their cofactor binding steps, and these steps have their own discrete microscopic rate constants. These microscopic rate constants may be rate-determining, depending on the reaction.

Unlike the WT enzyme, oxidation of androsterone by W227A under single-turnover conditions exhibits a k_{lim} value that is identical to the k_{cat} value. Furthermore, no burst phase was observed under multiple-turnover conditions. These two experimental findings demonstrate that mutation of W227 from a large hydrophobic residue to an alanine not only impedes substrate turnover but also alters the rate-determining step from product release to chemistry. Similar findings were observed for the F118A mutant. T226A exhibits transient kinetic parameters similar to those of WT with a k_{lim} value in single-turnover experiments considerably greater than k_{cat} and burst phase kinetics under multiple-turnover conditions. This mutation suggests that chemistry is not rate-limiting and that a product release event governs the rate-determining step, which is similar to that of the WT protein.

In previous studies, we have interpreted k_{cat} versus pH profiles for the WT and catalytic tetrad mutants on the assumption that k_{cat} was governed by the chemical step (*22*). While this new study may question the previous interpretation, we emphasize that our model for the chemical mechanism is still sound. First, the k_{cat} versus pH profiles previously determined were constructed using a different substrate pair, 5α-dihydrotestosterone and 3α-androstanediol, and the results on androsterone oxidation reported here may not be directly applicable. Second, these earlier studies showed that the single mutation which eliminated the titratable group with the maximum decrease in the pH-independent value of k_{cat} (10^5) was seen in the Y55F mutant in both the reduction and oxidation directions, supporting the role of Y55 as the general acid or base. Third, in acting as a general acid or base, Y55 used different neighboring residues, H117 or K84, respectively, to alter its ionization state. The H117A and K84M mutants also decreased k_{cat} significantly but only in the reduction and oxidation directions, respectively.

The dramatic effects seen on k_{cat} and not K_m or K_d by alanine scanning mutagenesis suggest that changes in the amino acid residues that line a steroid-binding pocket severely impede the catalytic power of the AKR. Alanine substitutions provide space in the binding site cavity where the ligands are no longer held in their most favorable orientation for the reaction to occur. This causes the steroid to wobble in the binding site, which in turn causes another microscopic step in the 3α-HSD mechanism to become rate-limiting. The highly conserved residues in the binding pocket of AKR1C enzymes (i.e., W227 and F118) are critical not only for steroid binding but also in positioning the steroid for participation in catalysis. The net effect of the alanine mutants was to disturb the positioning of the steroid substrate at the active site so that the chemical event becomes solely rate-determining.

The results of this alanine scanning mutagenesis study may have broad applicability to other steroid hormone-transforming enzymes and steroid binding proteins. They suggest that substitution of individual short polar residues or hydrophobic residues will have modest effects on affinity, but because the optimal positioning of steroid hormone may be affected, far greater effects on efficacy may be observed. For a steroid hormone-transforming enzyme, effects on k_{cat}, which overwhelm the effects on K_d, are anticipated. We speculate that for a steroid receptor, effects on the transactivation (efficacy/power) may overwhelm the effects on K_d, where the motion of the steroidal ligand within the binding site may influence the ligand-induced conformational change that recruits coactivators or corepressors.

ACKNOWLEDGMENT

We thank Dr. Dewey McCafferty and Dr. Marcos Milla for the use of the spectrofluorimeter.

SUPPORTING INFORMATION AVAILABLE

Steady-state kinetic data. This material is available free of charge via the Internet at http://pubs.acs.org.

REFERENCES

1. Labrie, F., Luu-The, V., Lin, S. X., Simard, J., Labrie, C., El-Alfy, M., Pelletier, G., and Belanger, A. (2000) Intracrinology:

role of the family of 17β-hydroxysteroid dehydrogenases in human physiology and disease, *J. Mol. Endocrinol. 25*, 1−16.
2. Labrie, F., Luu-The, V., Lin, S. X., Labrie, C., Simard, J., Breton, R., and Belanger, A. (1997) The key role of 17β-hydroxysteroid dehydrogenases in sex steroid biology, *Steroids 62*, 148−158.
3. Russell, D. W., and Wilson, J. D. (1994) Steroid 5α-reductase: two genes/two enzymes, *Annu. Rev. Biochem. 63*, 25−61.
4. Rizner, T. L., Lin, H. K., Peehl, D. M., Steckelbroeck, S., Bauman, D. R., and Penning, T. M. (2003) Human type 3 3α-hydroxysteroid dehydrogenase (aldo-keto reductase 1C2) and androgen metabolism in prostate cells, *Endocrinology 144*, 2922−2932.
5. Kakuta, Y., Pedersen, L. G., Carter, C. W., Negishi, M., and Pederson, L. C. (1997) Crystal structure of estrogen sulphotransferase, *Nat. Struct. Biol. 4*, 904−908.
6. Azzi, A., Rehse, P. H., Zhu, D. W., Campbell, R. L., Labrie, F., and Lin, S. X. (1996) Crystal structure of human estrogenic 17β-hydroxysteroid dehydrogenase complexed with 17β-estradiol, *Nat. Struct. Biol. 3*, 665−668.
7. Ghosh, D., Pletnev, V. Z., Zhu, D. W., Wawrzak, Z., Duax, W. L., Pangborn, W. L., Pangborn, W., Labrie, F., and Lin, S. X. (1995) Structure of human estrogenic 17β-hydroxysteroid dehydrogenase at 2.20 Å resolution, *Structure 3*, 503−513.
8. Bennett, M. J., Albert, R. H., Jez, J. M., Ma, H., Penning, T. M., and Lewis, M. (1997) Steroid recognition and regulation of hormone action: crystal structure of testosterone and $NADP^+$ bound to 3α-hydroxysteroid/dihydrodiol dehydrogenase, *Structure 5*, 799−812.
9. Penning, T. M., Mukharji, I., Barrow, S., and Talalay, P. (1984) Purification and properties of a 3α-hydroxysteroid dehydrogenase of rat liver cytosol and its inhibition by anti-inflammatory drugs, *Biochem. J. 222*, 601−611.
10. Penning, T. M. (1997) Molecular endocrinology of hydroxysteroid dehydrogenases, *Endocr. Rev. 18*, 281−305.
11. Penning, T. M., Bennett, M. J., Smith-Hoog, S., Schlegel, B. P., Jez, J. M., and Lewis, M. (1997) Structure and function of 3α-hydroxysteroid dehydrogenase, *Steroids 62*, 101−111.
12. Majewska, M. D., Harrison, N. L., Schwartz, R. D., Barker, J. L., and Paul, S. M. (1986) Steroid hormone metabolites are barbiturate-like modulators of the GABA receptor, *Science 232*, 1004−1007.
13. Majewska, M. D. (1992) Neurosteroids: endogenous bimodal modulators of the $GABA_A$ receptor. Mechanism of action and physiological significance, *Prog. Neurobiol. 38*, 379−395.
14. Griffin, L. D., and Mellon, S. H. (1999) Selective serotonin reuptake inhibitors directly alter activity of neurosteroidogenic enzymes, *Proc. Natl. Acad. Sci. U.S.A. 96*, 13512−13517.
15. Taurog, J. D., Moore, R. J., and Wilson, J. D. (1975) Partial characterization of the cytosol 3α-hydroxysteroid: $NAD(P)^+$ oxidoreductase of rat ventral prostate, *Biochemistry 14*, 810−817.
16. Jacobi, G. H., Moore, R. J., and Wilson, J. D. (1977) Characterization of the 3α-hydroxysteroid dehydrogenase of dog prostate, *J. Steroid Biochem. 8*, 719−723.
17. Jacobi, G. H., and Wilson, J. D. (1976) The formation of 5α-androstane-3α,17β-diol by dog prostate, *Endocrinology 99*, 602−610.
18. Lambert, J. J., Belelli, D., Venning, C. H., and Peters, J. A. (1995) Neurosteroids and $GABA_A$ receptor function, *Trends Pharmacol. Sci. 16*, 295−303.
19. Penning, T. M., Burczynski, M. E., Jez, J. M., Hung, C.-F., Lin, H.-K., Ma, H., Moore, M., Palackal, N., and Ratnam, K. (2000) Human 3α-hydroxysteroid dehydrogenase isoforms (AKR1C1−AKR1C4) of the aldo-keto reductase superfamily: functional plasticity and tissue distribution reveals roles in the inactivation and formation of male and female sex hormones, *Biochem. J. 351*, 67−77.
20. Hoog, S. S., Pawlowski, J. E., Alzari, P. M., Penning, T. M., and Lewis, M. (1994) Three-dimensional structure of rat liver 3α-hydroxysteroid/dihydrodiol dehydrogenase: a member of the aldo-keto reductase superfamily, *Proc. Natl. Acad. Sci. U.S.A. 91*, 2517−2521.
21. Bennett, M. J., Schlegel, B. P., Jez, J. M., Penning, T. M., and Lewis, M. (1996) Structure of 3α-hydroxysteroid/dihydrodiol dehydrogenase complexed with $NADP^+$, *Biochemistry 35*, 10702−10711.
22. Schlegel, B. P., Jez, J. M., and Penning, T. M. (1998) Mutagenesis of 3α-hydroxysteroid dehydrogenase reveals a "push-pull" mechanism for proton transfer in aldo-keto reductases, *Biochemistry 37*, 3538−3548.
23. Jin, Y., Stayrook, S. E., Albert, R. H., Palackal, N. T., Penning, T. M., and Lewis, M. (2001) Crystal structure of human type III 3α-hydroxysteroid dehydrogenase/bile acid binding protein complexed with $NADP^+$ and ursodeoxycholate, *Biochemistry 40*, 10161−10168.
24. Ratnam, K., Ma, H., and Penning, T. M. (1999) The arginine 276 anchor for NADP(H) dictates fluorescence kinetic transients in 3α-hydroxysteroid dehydrogenase, a representative aldo-keto reductase, *Biochemistry 38*, 7856−7864.
25. Jez, J. M., Schegel, B. P., and Penning, T. M. (1996) Characterization of the substrate binding site in rat liver 3α-hydroxysteroid/dihydrodiol dehydrogenase. The roles of tryptophans in ligand binding and protein fluorescence, *J. Biol. Chem. 271*, 30190−30198.
26. Lowry, O. H., Rosenbrough, J. J., Farr, A. J., and Randall, R. J. (1951) Protein measurement with the Folin phenol reagent, *J. Biol. Chem. 193*, 265−275.
27. Ehrig, T., Bohren, K. M., Prendergast, F. G., and Gabbay, K. H. (1994) Mechanism of aldose reductase inhibition: binding of $NADP^+$/NADPH and alrestatin-like inhibitors, *Biochemistry 33*, 7157−7165.
28. Stinson, R. A., and Holbrook, J. J. (1973) Equilibrium binding of nicotinamide nucleotides to lactate dehydrogenases, *Biochem. J. 131*, 719−728.
29. Wilkinson, G. N. (1961) Statistical estimations in enzyme kinetics, *Biochem. J. 80*, 324−332.
30. Askonas, L. J., Ricigliano, J. W., and Penning, T. M. (1991) The kinetic mechanism catalysed by homogeneous rat liver 3α-hydroxysteroid dehydrogenase. Evidence for binary and ternary dead-end complexes containing non-steroidal anti-inflammatory drugs, *Biochem. J. 278*, 835−841.
31. Deyashiki, Y., Tamada, Y., Miyabe, Y., Nakanishi, M., Matsuura, K., and Hara, A. (1995) Expression and kinetic properties of a recombinant 3α-hydroxysteroid/dihydrodiol dehydrogenase isoenzyme of human liver, *J. Biochem. 118*, 285−290.
32. Pongsawasdi, P., and Anderson, B. M. (1984) Kinetic studies of rat ovarian 20α-hydroxysteroid dehydrogenase, *Biochim. Biophys. Acta 799*, 51−58.
33. Trauger, J. W., Jiang, A., Stearns, B. A., and LoGrasso, P. V. (2002) Kinetics of allopregnanolone formation catalyzed by human 3α-hydroxysteroid dehydrogenase type III (AKR1C2), *Biochemistry 41*, 13451−13459.
34. Wilson, D. K., Bohren, K. M., Gabbay, K. H., and Quiocho, F. A. (1992) An unlikely sugar substrate site in the 1.65 Å structure of the human aldose reductase holoenzyme implicated in diabetic complications, *Science 257*, 81−84.
35. Grimshaw, C. E., Bohren, K. M., Lai, C.-J., and Gabbay, K. H. (1995) Human aldose reductase: rate constants for a mechanism including interconversion of ternary complexes by recombinant wild-type enzyme, *Biochemistry 34*, 14356−14365.
36. Penning, T. M., Jin, Y., Heredia, V. V., and Lewis, M. (2003) Structure−function relationships in 3α-hydroxysteroid dehydrogenases: a comparison of the rat and human isoforms, *J. Steroid Biochem. Mol. Biol. 85*, 247−255.
37. Heredia, V. V., Kruger, R. G., and Penning, T. M. (2003) Steroid-binding site residues dictate optimal substrate positioning in rat 3α-hydroxysteroid dehydrogenase (3α-HSD or AKR1C9), *Chem.-Biol. Interact. 143−144*, 393−400.

BI0499563